High purity isotopically enriched ^{70}Ge and ^{74}Ge single crystals: Isotope separation, growth, and properties

Kohei Itoh
University of California at Berkeley and Lawrence Berkeley Laboratory, Berkeley, California 94720

W. L. Hansen
Lawrence Berkeley Laboratory, Berkeley, California 94720

E. E. Haller
University of California at Berkeley and Lawrence Berkeley Laboratory, Berkeley, California 94720

J. W. Farmer
University of Missouri, Columbia, Missouri 65211

V. I. Ozhogin, A. Rudnev, and A. Tikhomirov
Russian Science Center, Kurchatov Institute, 123182 Moscow, Russia

(Received 30 November 1992; accepted 16 February 1993)

^{70}Ge and ^{74}Ge isotopes were successfully separated from natural Ge and zone purified. Several highly enriched, high purity ^{70}Ge and ^{74}Ge single crystals were grown by the vertical Bridgman method. The growth system was designed for reliable growth of low dislocation density, high purity Ge single crystals of very small weight (~4 g). A ^{70}Ge and a ^{74}Ge crystal were selected for complete characterization. In spite of the large surface to volume ratio of these ingots, both ^{70}Ge and ^{74}Ge crystals contain low electrically active chemical net-impurity concentrations of $\sim 2 \times 10^{12}$ cm^{-3}, which is two orders of magnitude better than that of ^{74}Ge crystals previously grown by two different groups.[1,2] Isotopic enrichment of the ^{70}Ge and the ^{74}Ge crystals is 96.3% and 96.8%, respectively. The residual donors and acceptors present in both crystals were identified as phosphorus and copper, respectively. In addition, less than 10^{11} cm^{-3} gallium, aluminum, and indium were found in the ^{70}Ge crystal.

I. INTRODUCTION

Along with the substantial progress in semiconductor science and technology, the control of the isotopic composition of semiconductor materials ("Isotope Engineering") is starting to attract attention. Several physical properties which are influenced by isotopic composition can be studied in isotopically controlled crystals.[1–9] Development of isotope engineered materials may become important in the future for the semiconductor industry. Application of the neutron transmutation doping technique[10] to isotopically controlled multilayer structures[11] or to isotopically controlled Si–Ge alloys may lead to superior doping control. Because many elements in the periodic table consist of a number of stable isotopes present in certain fractions, the isotopic composition of all standard semiconductor materials is predetermined and fixed unless a special isotope separation process is applied. To date only a few different types of isotopically enriched semiconductor crystals have been produced: ^{74}Ge single crystals,[1–3] ^{76}Ge single crystals,[4,5] and ^{12}C and ^{13}C diamond single crystals.[6–9] High purity and low dislocation density isotopically enriched ^{70}Ge, ^{73}Ge, and ^{74}Ge single crystals of larger size (~800 g each) have been grown most recently by the Czochralski method in our group.

In this paper we will describe the isotope separation, purification, growth, and characterization of chemically pure, isotopically enriched ^{70}Ge and ^{74}Ge single crystals of ~1 cm^3 in volume. The development of a growth system that produces high quality Ge crystals in small size was necessary for our future goal of growing Ge crystals containing mixed isotopes in controlled ratios. Consumption of separated Ge isotopes for this purpose must be minimized because mixing reverses the isotope separation, an extremely elaborate and costly process. The elimination of the use of a seed crystal is also important in order to conserve the high isotopic purity of the starting material. A detailed description of a seedless ~4 g high purity Ge crystal growth system will be given.

Germanium is currently used in a variety of semiconductor sensors and detectors. Purely doped Ge single crystals with compensation less than 1% can be grown with high crystalline perfection. Such crystals have been

used in the development of high responsivity, low noise far infrared photoconductive detectors.[12] Ultrapure Ge *p-i-n* diodes with volumes of up to several hundred cm^3 are used mostly in gamma ray spectroscopy.[13] Germanium crystals with natural isotopic compositions have been doped by the neutron transmutation doping (NTD) technique. They are widely used as phonon-mediated detectors for dark matter searches and neutrino physics,[14,15] and as thermistors for cosmic ray background measurements.[16]

As shown in Table I, natural Ge consists of five stable isotopes with well-known relative abundances.[17] Among these isotopes, the ^{70}Ge and ^{74}Ge isotopes were chosen for this work because they become doped with shallow level impurities through NTD.[18] By exposing ^{70}Ge and ^{74}Ge crystals to a flux of thermal neutrons, ^{70}Ge crystal will become Ga doped, i.e., *p*-type due to the $^{70}\text{Ge} + n \rightarrow {}^{71}\text{Ge} + e \rightarrow {}^{71}\text{Ga}$ electron capture reaction, while the ^{74}Ge crystal will turn *n*-type due to the $^{74}\text{Ge} + n \rightarrow {}^{75}\text{Ge} \rightarrow {}^{75}\text{As}$ β-decay reaction. The NTD technique is known to produce the most homogeneous dopant distribution down to the atomic level.[10] ^{70}Ge and ^{74}Ge crystals described in this work are currently used in a variety of experiments.[19,20]

II. ISOTOPE SEPARATION PROCESS

Growth of isotopically enriched crystals requires isotopically separated starting materials in the elemental form in large enough quantities for zone refining. Ge isotope production in kilogram quantities was originally motivated by the search for the double β-decay in ^{76}Ge crystals.[4,5] The gas centrifuge system, which was used in the former Soviet Union for the uranium isotope enrichment, was also employed for the ^{76}Ge isotope separation.[21] An excellent review of this technique has been given by Olander.[22] In the past nine years, more than 26 kg of ^{76}Ge isotope with 85% enrichment (see Table I) was produced at the Kurchatov Institute of Atomic Energy (now the Russian Science Center "Kurchatov Institute").

In the germanium isotope separation process, volatile, chemically reactive germanium tetrafluoride (GeF_4) was used as a working gas. Its molecular mass is 149 AMU which is substantially smaller than that of uranium hexafluoride (353 AMU). A special modification of the gas centrifuge was needed in order to accommodate these significantly lighter molecules.[21] Germanium tetrafluoride enriched with the target isotope was transformed into germanium oxide GeO_2 followed by its reduction to the elemental form.

Enriched ^{70}Ge can be produced directly from natural Ge since it is the lightest stable isotope of Ge. On the other hand, the second heaviest stable isotope ^{74}Ge may be efficiently separated only from an isotope mixture with a minimal content of the heaviest ^{76}Ge component. After the removal of ^{76}Ge, the remaining mixture (^{76}Ge content of only about 1.2%) was used to separate the ^{74}Ge isotopes. Several hundred grams of ^{70}Ge and ^{74}Ge isotopes with enrichments shown in Table I have been produced at the Kurchatov Institute and have been made available to a number of research groups in Russia, the Ukraine, and the United States.

TABLE I. Isotopic composition of the Ge isotopes enriched at the Kurchatov Institute.

	Isotope				
Isotopic product	^{70}Ge	^{72}Ge	^{73}Ge	^{74}Ge	^{76}Ge
Natural Ge	20.5%	27.4%	7.8%	36.5%	7.8%
^{76}Ge	0.1%	0.1%	0.2%	14.5%	85.1%
^{74}Ge	0.1%	0.9%	3.8%	92.6%	2.6%
^{70}Ge	96.3%	2.1%	0.1%	1.2%	0.3%

III. ZONE PURIFICATION

We started our zone purification process with 100 g each of isotopically enriched granular powders of ^{70}Ge and ^{74}Ge. The donor concentration in the powder was so high that the Ge crystal grown from this material with no purification process exhibited metallic conduction (free electron concentration $> 3 \times 10^{17}$ cm^{-3}). Each of the isotopically enriched ^{70}Ge and ^{74}Ge powders was contained in a crucible of ultrapure graphite.[23] The crucible was placed in a quartz tube which allowed atmosphere control. After each powder was transformed into a very narrow continuous Ge polycrystalline bar (~50 cm long, ~0.4 cm^2 cross section area), a short molten zone (2.5 cm long) was formed by a RF coil. The liquid zone traveled from one end of the bar to the other at a steady speed of 10 cm/h in a continuous flow of forming gas (90% N_2 and 10% H_2 mixture). Careful adjustment of the RF heater power and the tilt angle of the bar was necessary in order to keep the narrow Ge bar from breaking up into a string of drop-shaped pieces. The removal of a small piece from the impure end of the bar after every ten zone passes decreased the total amount of impurities in the bar by 1–2 orders of magnitude. After completion of 25 zone passes, the net electrically active impurity concentration profile along the direction of the zone-refined polycrystalline bar was determined via a resistivity measurement at 77 K in the dark at 7 cm intervals. The net-impurity concentration $|N_A - N_D|$ can be calculated with the relation $|N_A - N_D| = 1/\rho\mu q$, where N_A and N_D are the ionized acceptor and donor impurity concentrations per cm^3, respectively, μ is the mobility (~40 000 cm^2/Vs for both electrons and holes in pure Ge at 77 K), and q is the electron charge (1.6×10^{-19} C). Figure 1 shows the net-impurity concentration

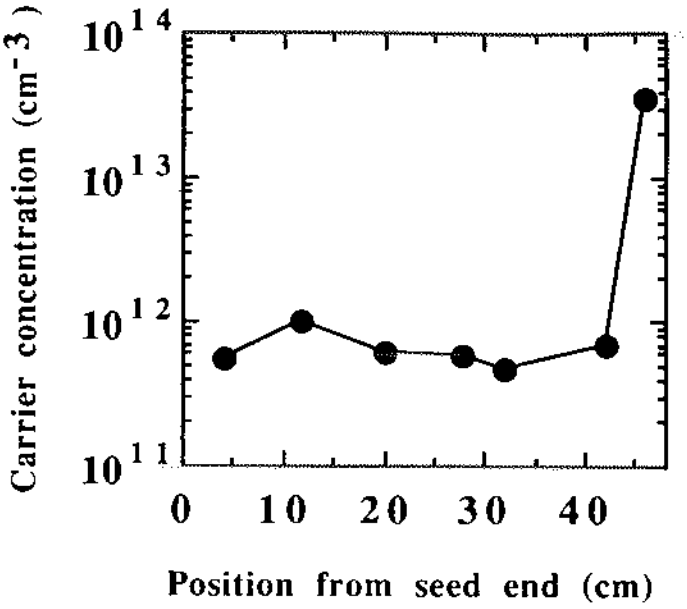

FIG. 1. Net carrier concentration profile of the ^{70}Ge polycrystalline bar after 25 zone-refining passes.

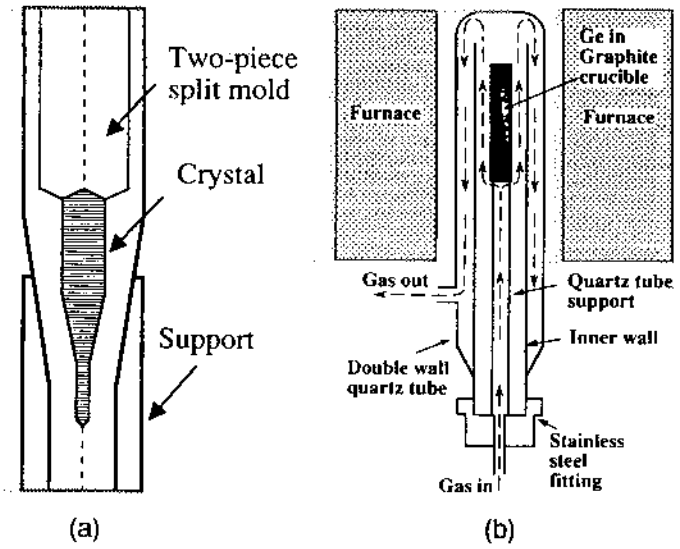

FIG. 2. (a) Cross section schematic of the split graphite crucible. (b) Schematic of the seedless vertical Bridgman Ge crystal growth system.

profile of the ^{70}Ge refined bar after 25 zone passes. More than 80% of the bar was purified to $|N_A - N_D| < 10^{12}$ cm^{-3}. This value corresponds to the highest degree of the purification one can measure from the purest graphite crucibles[24] due to defects and impurities at grain boundaries and dislocations. The net-impurity concentration profile of the ^{74}Ge zone-refined bar is almost identical to the ^{70}Ge bar.

IV. CRYSTAL GROWTH

The crystal growth apparatus developed for this work is specifically designed for ease of handling and rapid high purity growth of Ge single crystals of ~4 g in weight. The growth direction of the crystal cannot be predetermined because it is a seedless growth system which fully conserves the isotopic enrichment. The ability to control some important parameters for crystal growth (growth rate, interface temperature gradient, etc.) is limited because of the small dimension of the system. Nevertheless, with empirically determined parameters, we can reliably grow high-quality Ge single crystals in less than 6 h. Figure 2 shows the schematics of the ultrapure graphite split crucible (a) and of the growth system (b). Prior to crystal growth, the interior of the crucible[23] is coated with a ~20 μm thick carbon soot formed by an oxygen-starved high purity butane (C_4H_{10}) flame. The soft carbon layer suppresses the sticking of Ge to the crucible. Carbon is of no concern regarding purity because it is a neutral impurity in Ge, and its solubility is ~10^{14} cm^{-3} near the melting point.[25]

The crucible containing Ge starting material is placed inside the double-wall quartz tube. One end of the double-wall quartz tube is closed, and crucible loading and gas feeding are performed through the open end. The dimensions of the outer tube are roughly 3 cm for the diameter and 50 cm for the length. The open end of the quartz tube is sealed by an "Ultra-torr" stainless steel fitting manufactured by Swagelock Corporation, USA. The crucible rests on the inner quartz support that is standing on the stainless steel fitting. The quartz tube is positioned inside the vertical furnace such that the crucible sits at a well-calibrated position of the furnace. During the growth process, forming gas is fed (mixture of N_2 ~ 1 l/min and H_2 ~ 200 cc/min) through the gas inlet valve in order (1) to avoid oxidation and (2) to passivate impurities with hydrogen. The gas travels along the path shown by the arrows in Fig. 2(b) and exits through the gas outlet valve. After the germanium inside the crucible has been melted completely, the furnace temperature is slowly lowered (~2 °C/min). At the same time the flow rate of the gas is increased so that the cold gas reaching the bottom of the crucible creates an appropriate temperature gradient for upward single-crystal growth. The grown crystal can be taken out simply by disassembling the split crucible. Figure 3 shows a photograph of the isotopically enriched ^{70}Ge and ^{74}Ge crystals grown by the method described above. An 18 mm diameter United States ten-cent coin is shown to give a scale. Both crystals are about 4 g in weight, 6.5 mm in diameter, and 4.5 cm in length.

V. CHARACTERIZATION OF ISOTOPICALLY ENRICHED ^{70}Ge AND ^{74}Ge SINGLE CRYSTALS

Several ^{70}Ge and ^{74}Ge crystals were grown, and one ingot from each ^{70}Ge and ^{74}Ge crystals was selected for

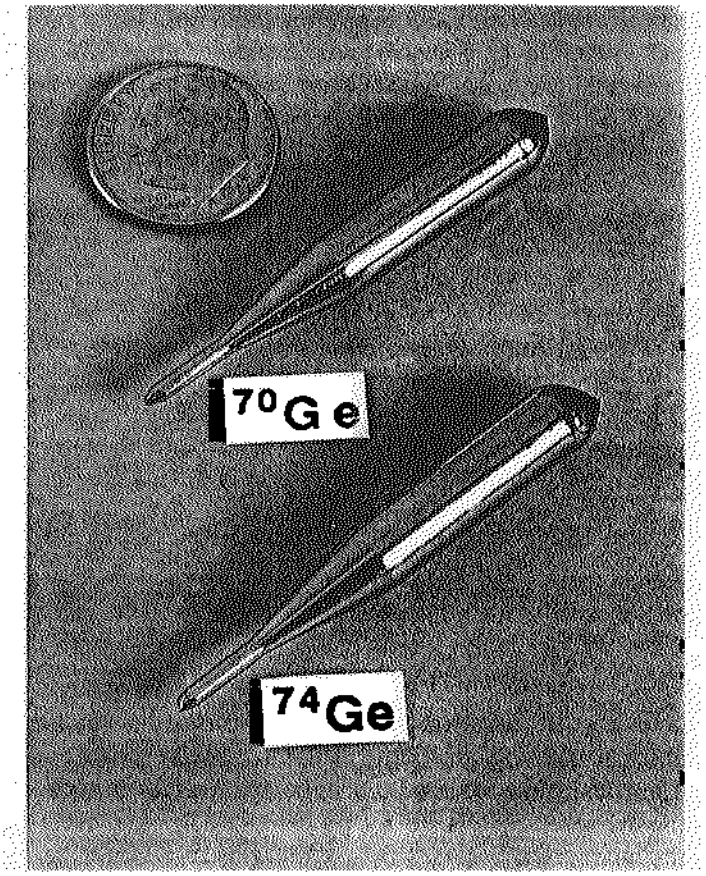

FIG. 3. Isotopically enriched ^{70}Ge and ^{74}Ge single crystals.

full analysis. We believe the following characterization results on these two crystals represent the rest of the ^{70}Ge and ^{74}Ge crystals since they were grown under identical conditions. First, each of the ^{70}Ge and ^{74}Ge ingots was confirmed to be single crystal, even though the seedless growth relies on random nucleation at the very bottom of the crucible.

A. Isotopic composition

The isotopic composition of ^{70}Ge and ^{74}Ge crystals was found by secondary ion mass spectrometry (SIMS). Both crystals displayed exactly the same composition as that of their respective starting materials shown in Table I. This showed that the conservation of isotopic purity with our seedless growth system was successful, and both crystals had an isotopic enrichment of over 96%.

B. Crystal orientation measurement (optical reflection technique)

The crystallographic orientation of these crystals was not predetermined due to our seedless growth system. Optical reflection patterns, obtained from the {111} planes formed on the rough-lapped surfaces which were preferentially etched with $HF:H_2O_2:H_2O = 1:1:4$ solution, were used to determine the direction of both crystals. The growth axes of ^{70}Ge and ^{74}Ge were found to lie near ⟨179⟩ and ⟨249⟩, respectively. Prior to the growth of the isotopically enriched crystals, more than seventy natural Ge crystals had been grown by the same seedless method. After statistical examination of the orientation distribution of these crystals, the ⟨113⟩ direction was found to be the preferred growth direction of crystals grown with this system. Indeed, the ^{74}Ge crystal growth axis lies near ⟨113⟩. However, there were some exceptions as one can see in the case of ^{70}Ge.

C. Net-impurity concentration profile

The net-impurity concentration profiles in both crystals were found from resistivity measurements described in the previous zone purification section. The results for both ^{70}Ge and ^{74}Ge crystals displayed in Fig. 4 show that more than 70% of each crystal have a net-impurity concentration of the order of 10^{12} cm^{-3}. It was also found that ^{74}Ge is entirely p-type whereas ^{70}Ge contains a p-n-junction and is p-type near the growth tail end. The identities of the dominant residual impurities will be discussed in the following sections.

D. Temperature dependence of the free carrier concentration

The temperature dependence of the free carrier concentration of four wafers cut from the ^{70}Ge and ^{74}Ge

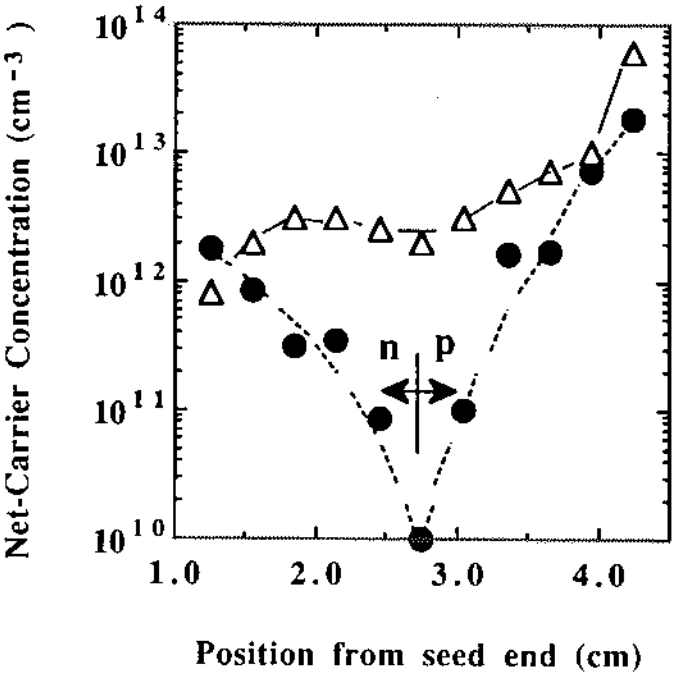

FIG. 4. Net-impurity concentration profile in ^{70}Ge (●) and ^{74}Ge (△) crystals.

crystals was investigated by using the variable temperature Hall effect technique. Figure 5 shows the temperature dependent free carrier concentration of two wafers cut from ^{74}Ge. Wafers ^{74}Ge-18 and ^{74}Ge-42 were cut at 1.8 cm and 4.2 cm from the seed end, respectively. They are both *p*-type, and their net-impurity concentrations, 2×10^{12} cm^{-3} for ^{74}Ge-18 and 1×10^{14} cm^{-3} for ^{74}Ge-42, agree very well with the resistivity measurement shown in Fig. 4. From the slope of the freeze-out curve, the ionization energy of a majority *p*-type impurity in both samples was calculated to be ~40 meV. Comparing this result with the list of ionization energies for various acceptors in Ge,[26] we found copper (listed value 43 meV) to be the most likely majority impurity. The compensating donor concentration in ^{74}Ge-42 samples was found to be 3×10^{11} cm^{-3} from the change in slope in the freeze-out region. The ^{74}Ge-18 freeze-out curve shows no half-slope regions, which indicates that the donor level concentration in this sample lies between 10^{11} and 10^{12} cm^{-3}.

Figure 6 shows the Hall effect result of two wafers cut from crystal ^{70}Ge. In this case, ^{70}Ge-18 is *n*-type and ^{70}Ge-42 is *p*-type. The carrier freeze-out region of ^{70}Ge-18 could not be measured due to the failure of the *n*-type ohmic contacts below 20 K. However, it can be still concluded that the net-impurity concentration of ^{70}Ge-18 is 2×10^{12} cm^{-3}, and the majority impurity is one of the shallow donors since the curve does not freeze out above 20 K. The ^{70}Ge-42 curve shows two big steps, suggesting the presence of both shallow and deep acceptors. The concentration of the deep acceptors is 7×10^{13} cm^{-3} and of the shallow acceptors is 5×10^{12} cm^{-3}. Net-impurity concentration results on ^{70}Ge-18 and ^{70}Ge-42 obtained by the Hall effect are also in good agreement with the resistivity results shown in Fig. 4. The ionization energy of the shallow acceptor calculated from the slope is 12.4 meV, which is a typical value predicted by the effective mass theory for hydrogenic acceptor impurities. It is not possible to identify the half-slope region in the freeze-out curve. This indicates that the compensating donor concentration is rather close to the majority shallow impurity concentration of 5×10^{12} cm^{-3}.

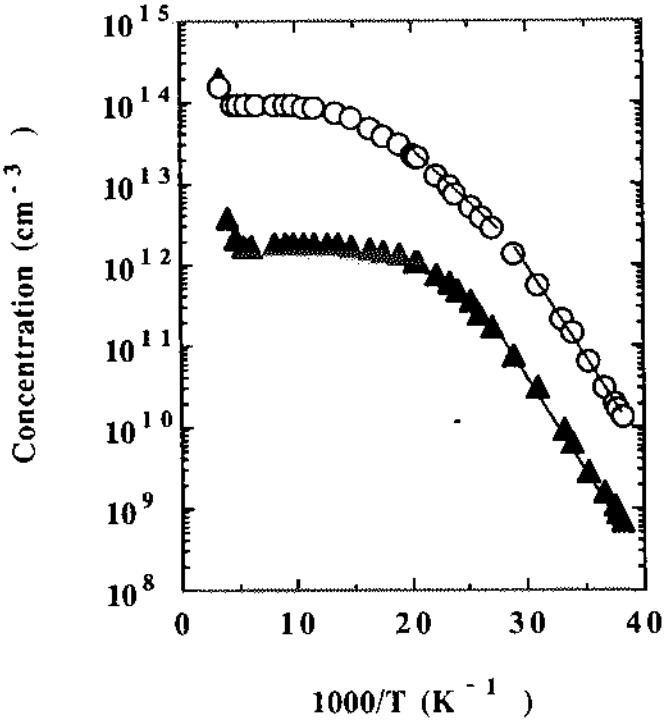

FIG. 5. Arrhenius plot of the free carrier concentration and the absolute temperature of the ^{74}Ge-18 (○) and ^{74}Ge-42 (▲) samples.

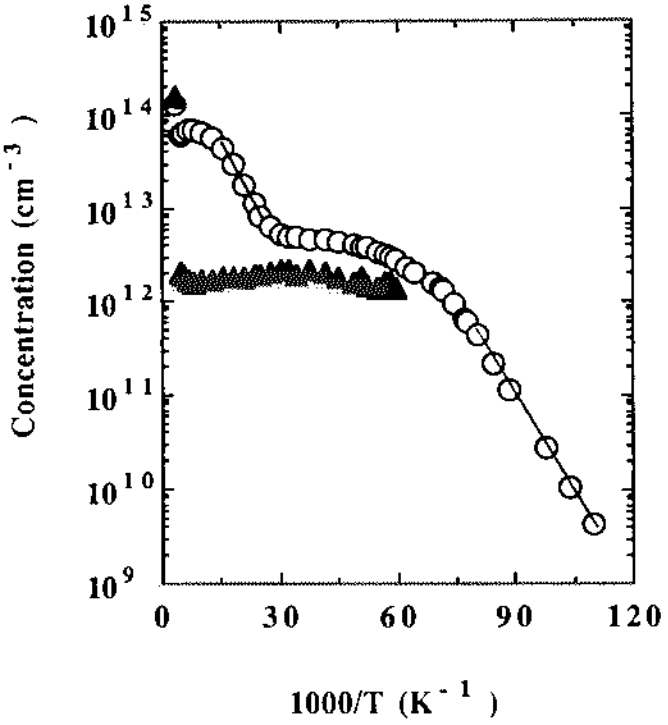

FIG. 6. Arrhenius plot of the free carrier concentration and the absolute temperature of the ^{70}Ge-18 (○) and ^{70}Ge-42 (▲) samples.

E. Impurity identification with photothermal ionization spectroscopy (PTIS)

PTIS was employed to identify the electrically active impurities in the crystals ^{70}Ge and ^{74}Ge. This technique is known to be extremely sensitive, offering detection limits of less than 10^{8} cm^{-3} shallow impurities in favorable cases.[13,27] Figure 7 shows the PTIS spectrum obtained with ^{74}Ge-42. The positions of the three major peaks correspond exactly to the B, C, and D transition line energies of neutral copper. This confirms unambiguously the presence of copper, consistent with the result of the Hall effect measurements. No peaks due to other

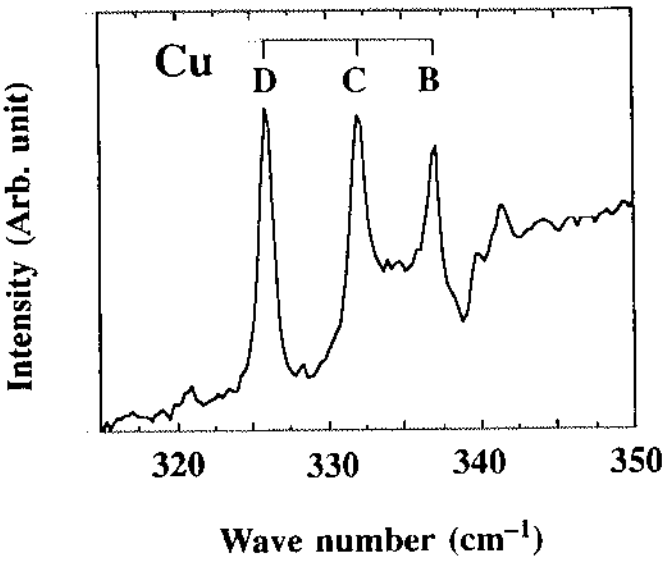

FIG. 7. PTI spectrum of sample ^{74}Ge-42.

semideep acceptors (Be, Zn) were observed with PTIS. Copper peaks were also observed in sample ^{70}Ge-42.

Figure 8 shows the PTIS spectrum of ^{70}Ge-18. As seen in Fig. 6, this sample is *n*-type with the net-impurity concentration of $\sim 2 \times 10^{12}$ cm^{-3}. The strong peak at 90 cm^{-1} confirms the presence of phosphorus. Phosphorus was found also in the ^{74}Ge crystal. Because phosphorus and copper were detected in most natural Ge crystals grown in the same system, their source is thought to lie in the growth system rather than in the starting material. Further PTIS studies identified the shallow acceptors in ^{70}Ge-42. They are $\sim 10^{12}$ cm^{-3} aluminum with smaller amounts ($< 10^{11}$ cm^{-3}) of gallium and indium.

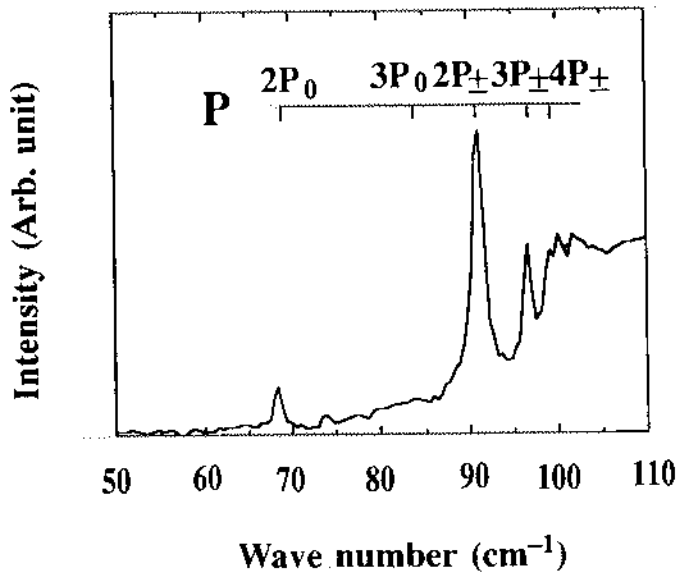

FIG. 8. PTI spectrum of sample ^{70}Ge-18.

F. Dislocation density

The dislocation distributions in the ^{70}Ge and ^{74}Ge crystals were found by means of preferential chemical etching. The ^{74}Ge crystal has 10^2–10^3 cm^{-2} dislocations distributed rather homogeneously. The ^{70}Ge crystal possesses a similar distribution with slightly higher density, 10^3–10^4 cm^{-2}. The study of dislocation distributions along the crystal axis indicates the following potential sources for dislocations: (1) External stress arising from the sticking of the solidifying Ge to the inner wall of the crucible, (2) gas bubbles contained in the Ge liquid acting as stress sources during the solidification, and (3) carbon particles contained in the Ge liquid that are not able to escape to the surface during the Ge solidification. The direction of the growth axes was found to be another important factor for the elimination of dislocations. Pure edge dislocations in Ge have a Burgers vector along ⟨110⟩. Once dislocated regions are created, the propagation behavior of dislocations depends on the growth direction. As stated in the last section, ⟨113⟩ is the statistically most preferred growth direction. In this case dislocation lines are 30° off the growth axis, and dislocations can grow out of the crystal. On the other hand, some crystals have their axes very close to the ⟨110⟩ orientation. Indeed this was the case for the ^{70}Ge crystal in which a slightly higher dislocated spot propagates along the growth axis all the way to the end. Most crystals with their growth axis near ⟨110⟩ contain slightly higher dislocation densities.

VI. SUMMARY

We have successfully grown high purity, isotopically enriched ^{70}Ge and ^{74}Ge single crystals. Table II shows the summary of the characterization results on the ^{70}Ge and the ^{74}Ge crystal. The most important property, the "isotopic enrichment," was found to be over 96% in both crystals. In spite of the very small size of the ingots (i.e., unfavorable surface to volume ratio for a high-purity crystal growth), nearly 75% of both crystals contain 2×10^{12} cm^{-3} residual net impurities which is two orders of magnitude less than those of the ^{74}Ge enriched crystals grown previously. This was achieved by the zone purification and careful cleaning and maintenance of the crystal growth system. Although we achieved quite low dislocation densities ($\sim 10^3$ cm^{-2}) in both ^{70}Ge and ^{74}Ge ingots, further improvement in dislocation distribution is desirable. Both crystals were found to contain a small concentration of copper impurities (2×10^{12} cm^{-3}). The source of Cu in our growth system is currently being investigated.

Lastly, we have recently grown an isotopically controlled Ge single crystal containing ^{70}Ge and ^{76}Ge isotopes in a one to one ratio with the system described in this paper. Our preliminary isotopic composition mea-

TABLE II. Summary of characterization results on the ^{70}Ge and ^{74}Ge crystals.

Crystal	^{70}Ge	^{74}Ge
Isotopic enrichment	96.3%	96.8%
Orientation	⟨179⟩	⟨249⟩
Dislocation density	10^3–10^4 cm^{-2}	10^2–10^3 cm^{-2}
Net-impurity concentration (Pure side of the crystal)	2×10^{12} cm^{-3}	2×10^{12} cm^{-3}
Type (n or p)	n	p
Majority impurity	P	Cu
Minority impurity	[Cu] $< 10^{12}$ cm^{-3}	[P] $< 10^{12}$ cm^{-3}
Other impurities (Total less than 10^{11} cm^{-3})	...	Al, Ga, In

surement by SIMS shows that both isotopes distributed homogeneously throughout the crystal. We are planning to grow ~4 g Ge single crystals of various isotopic composition in the near future.

ACKNOWLEDGMENTS

We are indebted to J. Beeman for helpful discussions and technical support. This work was supported in part by the United States NSF Center for Particle Astrophysics ADT-8809616 and in part by the United States NASA Contract W17605 through interagency agreement with the United States Department of Energy Contract DE-AC03-76SF00098.

REFERENCES

1. I.S. Shlimak, L.I. Zarubin, A.N. Ionov, F.M. Vorobkalo, A.G. Zabrodskii, and I.Y. Nemish, Sov. Tech. Phys. Lett. **9**, 377 (1983).
2. T.H. Geballe and G. Hull, Phys. Rev. **110**, 773 (1958).
3. R.C. Buschert, A.E. Merlini, S. Pace, S. Rodriguez, and M.H. Grimsditch, Phys. Rev. B **38**, 5219 (1988).
4. A.A. Vasenko, Yu. I. Vereshchagin, I.V. Kirpichnikov, V.A. Kuznetsov, V.N. Prusakov, A.I. Rudnev, A.S. Starostin, and A.V. Tikhomirv, Prib. Tekh. Eksp. **N2**, 56 (1989), in Russian [Instrum. Exp. Tech. **32**, 312 (1989)].
5. CERN Courier **31**, 14 (1991).
6. T.R. Anthony, W.F. Banholzer, J.F. Fleischer, L. Wei, P.K. Kuo, R.L. Thomas, and R.W. Pryor, Phys. Rev. B **42**, 1104 (1990).
7. A.T. Collins, S.C. Lawson, G. Davies, and H. Kanda, Phys. Rev. Lett. **65**, 891 (1990).
8. A.T. Collins, S.C. Lawson, G. Davies, and H. Kanda, Mod. Phys. Lett. B **5**, 407 (1991).
9. H. Holloway, K.C. Hass, M.A. Tamor, T.R. Anthony, and W.F. Banholzer, Phys. Rev. B **44**, 7123 (1991).
10. *Neutron Transmutation Doping of Semiconductor Materials*, edited by R.D. Larrabee (Plenum, New York, 1984).
11. E.E. Haller, Semicond. Sci. Technol. **5**, 319 (1990).
12. N.M. Haegel, M.R. Hueschen, and E.E. Haller, Infrared Phys. **25**, 273 (1985).
13. E.E. Haller and F.S. Goulding, in *Handbook of Semiconductors*, Chap. 6c, edited by C. Hilsum (North-Holland, Amsterdam, 1980), Vol. 4, p. 799, second edition in press.
14. N. Wang, B. Sadoulet, T. Shutt, J. Beeman, E.E. Haller, A. Lange, I. Park, R. Ross, C. Stanton, and H. Steiner, IEEE Trans. Nucl. Sci. **NS-35**, No. 1, 55 (1988).
15. B. Sadoulet, T. Shutt, N. Wang, A. Commings, P. Barnes, J. Beeman, J. Emes, Y. Giraud-Heraud, E.E. Haller, A. Lange, J. Rich, and R. Ross, in *Low Temperature Detectors for Neutrinos and Dark Matter III*, edited by L. Brogiato, D.V. Camin, and E. Fiorini (Editions Frontiers, Gif sur Yvette, 1990), p. 227.
16. A.E. Lange, E. Kreysa, S.E. McBride, P.L. Richards, and E.E. Haller, Int. J. IR MM Waves **4**, 689 (1983).
17. *Table of Isotopes*, 7th ed., edited by C.M. Lederer and V.S. Shirley (John Wiley & Sons, New York, 1978).
18. E.E. Haller, N.P. Palaio, M. Rodder, W.L. Hansen, and E. Kreysa, *Neutron Transmutation Doping of Semiconductor Materials*, edited by R.D. Larrabee (Plenum, New York, 1984), p. 21.
19. H.D. Fuchs, C.H. Grein, C. Thomsen, M. Cardona, W.L. Hansen, E.E. Haller, and K. Itoh, Phys. Rev. B **43**, 4835 (1991).
20. G. Davies, E. Lightowlers, K. Itoh, W.L. Hansen, and E.E. Haller, Proc. 5th Int. Conf. on Shallow Impurities in Semiconductors, Kobe, Japan (1992, in press).
21. E.I. Abbakumov, V.A. Bazhenov, Yu. V. Verbin, A.A. Vlasov, A.S. Dorogobed, A.K. Kaliteevskii, V.F. Kornilov, D.M. Levine, E.I. Mikerin, A.A. Sazykin, V.I. Sergeev, and G.S. Soloviev, At. Energ. **67**, 255 (1989), in Russian [Sov. J. At. Energy **67**, 739 (1989)].
22. D.R. Olander, Sci. Am. **239**, 37 (1978).
23. The graphite boat and crucible were made and purified by Carbon USA, Ultra Carbon Division, USA.
24. G.S. Hubbard, E.E. Haller, and W.L. Hansen, Nucl. Instrum. Methods **130**, 481 (1978).
25. E.E. Haller, W.L. Hansen, P.N. Luke, R. McMurray, and B. Jarrett, IEEE Trans. Nucl. Sci. **NS-29**, No. 1, 745 (1982).
26. M.S. Skolnick, in *Landolt-Börnstein Data Series III* (Springer, Berlin, 1989), Vol. 22b, p. 466.
27. Sh. M. Kogan and T.M. Lifshits, Phys. Status Solidi A **39**, 11 (1977).